ELSEVIER

Polymer 43 (2002) 4087–4090

polymer

www.elsevier.com/locate/polymer

Polymer Communication

Size dependence of crystallization within spherical microdomain structures

Shuichi Nojima[a,*], Masashi Toei[a], Shigeo Hara[b], Satoshi Tanimoto[b], Shintaro Sasaki[b]

[a]*Department of Polymer Chemistry, Tokyo Institute of Technology, 2-12-1 Ookayama, Meguro-Ku, Tokyo 152-8552, Japan*
[b]*School of Materials Science, Japan Advanced Institute of Science and Technology (JAIST), Tatsunokuchi, Ishikawa 923-1292, Japan*

Received 17 January 2002; received in revised form 8 March 2002; accepted 18 March 2002

Abstract

We have investigated the size dependence of crystallization within spherical microdomains formed in various poly(ε-caprolactone)-*block*-polybutadiene diblock copolymers (PCL-*b*-PB). The crystallinity (χ) and melting temperature (T_m) of the PCL block are considerably lower than those of PCL homopolymer, and χ decreases steadily and T_m decreases only slightly with decreasing radius of PCL spheres (R) for a series of PCL-*b*-PB with a same molecular weight (M_n). When PCL-*b*-PB is compared with the similar R but different M_n, χ is significantly different, suggesting that the sphere size is not the unique factor to control crystallization within spherical microdomains.

Keywords: Spherical microdomain; Crystallization; Size dependence

1. Introduction

The interplay between crystallization and microphase separation has a possibility to provide a wide variety of morphologies in polymer systems. That is, the pre-existing microdomain structure affects intimately the subsequent crystallization to result in extremely different morphologies such as crystallized microdomain structure or lamellar morphology, an alternating structure consisting of lamellar crystals and amorphous layers. This difference depends critically both on the stability (or segregation strength) of microdomain structures in the melt and the mobility of constituent copolymers [1].

Recently, much attention has been paid to the crystallization within spherical or cylindrical microdomains because the curved interface of microdomains seems to be incompatible with the crystal structure. In addition, spherically or cylindrically confined nanophase may change the crystallization behavior and eventually final morphology compared with the case of homopolymer crystallization. Crystallization within nanosize spheres was recently confirmed by Loo et al. [2] with a polyethylene-*block*-poly(styrene-*ran*-ethylene-*ran*-butene) copolymer, where the crystallization behavior was extremely different from that of homopolymer. Chen et al. [3] showed that the degree of supercooling necessary for crystallization depends significantly on the type of microdomain structures existing in the melt.

In this communication, we report the size dependence of crystallization within spherical microdomains. That is, the crystallinity and melting temperature of spherically confined crystalline blocks were measured as a function of the radius of spherical microdomains to understand the characteristics of crystallization within nanosize spheres. The samples employed here are poly(ε-caprolactone)-*block*-polybutadiene copolymers (PCL-*b*-PB) which have spherical microdomain structures in the melt with the PCL block inside. The crystallization of PCL blocks was confirmed by wide-angle X-ray diffraction (WAXD) and differential scanning calorimetry (DSC), the morphology before and after crystallization was probed by small-angle X-ray scattering (SAXS), and the crystallinity (χ) and melting temperature (T_m) of PCL blocks were evaluated by DSC. From these results, we discuss the size dependence of crystallization confined within spherical microdomains.

2. Experimental

PCL-*b*-PB copolymers were synthesized by a successive anionic polymerization under vacuum. Details of the synthesis and purification are described elsewhere [4,5]. The molecular characteristics of PCL-*b*-PB are shown in

* Corresponding author. Tel.: +81-3-5734-2132; fax: +81-3-5734-2888.
E-mail address: snojima@polymer.titech.ac.jp (S. Nojima).

0032-3861/02/$ - see front matter
PII: S0032-3861(02)00217-3

Table 1
Molecular characteristics of PCL-*b*-PB copolymers used in this study

Notation	Total M_n[a]	M_n (PCL)[b]	M_w/M_n[c]	PCL/PB (vol%)[d]	R_s (nm)[e]	R_p (nm)[f]
B100-3	100,000	4000	1.09	3:97	10.3	–
B100-8	100,000	10,000	1.13	8:92	15.1	14.5
B100-17	100,000	20,000	1.12	17:83	17.4	17.3
B62-6	62,000	5000	1.13	6:94	11.1	11.6
PCL[g]	6500	6500	1.20	100:0	–	–

[a] Determined by membrane osmometer.
[b] Calculated from the values of total M_n and PB block M_n.
[c] Determined by GPC.
[d] Determined by ^{1}H-NMR.
[e] Calculated from the SAXS peak position and PCL volume fraction.
[f] Calculated from the angular position of the particle scattering maximum.
[g] Obtained from Polymer Source Inc. and molecular parameters are provided by the manufacturer.

Table 1, where the first number in 'notation' represents the total molecular weight (M_n, kg/mol) and the second one represents volume percent of PCL blocks in the copolymer. The volume fraction of PCL blocks is suppressed to less than 0.17 in order to get spherical microdomains in the melt. We investigate mainly the size dependence of crystallization for the same molecular weight samples (B100-3, B100-8, and B100-17), and we use B62-6 to investigate the M_n dependence of crystallization with the similar size of PCL spheres. PCL homopolymer, which was used to compare the crystallization behavior with PCL-*b*-PB, was purchased from Polymer Source Inc. and the molecular parameters are provided by the manufacturer.

The morphology formed in the melt and after crystallization was investigated by SAXS. Details of the apparatus and measurement conditions are described elsewhere [6]. The scattered intensity was corrected for the background scattering and the absorption by the sample, and relative intensities are obtained as a function of wave number s defined as $s = (2/\lambda)\sin\theta$, where λ is the wavelength of X-ray (=0.1542 nm) and 2θ is the scattering angle.

The radius of PCL spheres in the microdomain structure was calculated by two independent methods (denoted as R_s and R_p); R_s was calculated from the volume fraction of PCL blocks in the copolymer and the angular position of the SAXS intensity maximum arising from a regular microdomain structure with a body-centered cubic (BCC) lattice, and R_p from the angular position of the broad scattering appearing from the form factor of isolated spheres by using the following equation

$$I(s) = \left[\frac{3(\sin x - x\cos x)}{x^3}\right]^2 \qquad \text{with } x = 2\pi s R_p \tag{1}$$

and

$$2\pi s_{max} R_p = 5.76, \ldots \tag{2}$$

where s_{max} is the angular position of the broad intensity maximum from isolated spheres.

Crystallization in spherical microdomains was confirmed by two methods: WAXD from PCL crystals and the exothermic heat by DSC when the sample was gradually cooled. WAXD was performed with Rigaku diffractometer (RAXIS 200IIC) using Ni-filtered Cu Kα radiation supplied by a Rigaku RU300 generator operating at 40 kV and 100 mA. Details of the apparatus are described elsewhere [7]. The DSC experiment was carried out with Perkin Elmer Pyris 1 DSC with a cooling rate of 5 °C/min.

The melting temperature T_m and the crystallinity of PCL chains χ were evaluated by DSC. The sample was first kept at approximately 65 °C for 30 min and followed by quenching into various crystallization temperatures T_c ranging from −40 to −60 °C for PCL-*b*-PB and from 30 to 45 °C for PCL, and then heated at a rate of 5 °C/min to get the endothermic peak by the melting of PCL chains. T_m was defined by the maximum temperature of the endothermic peak and χ was calculated from the peak area ΔH (J/g) by

$$\chi = \Delta H/(\Delta H^* f_w) \times 100 \tag{3}$$

where f_w is the weight fraction of PCL blocks in PCL-*b*-PB and ΔH^* is the heat of fusion for perfect PCL crystals ($\Delta H^* = 135.44$ J/g [8]). Though χ and T_m of PCL were slightly increased at a later stage of crystallization with increasing crystallization time t, and those of PCL-*b*-PB became constant after a relatively short t (<100 min) in the T_c range employed ($-60 \le T_c \le -40$ °C). The constant values of χ and T_m were evaluated by plotting χ (and T_m) against t at each T_c for individual sample. Therefore χ and T_m reported here are final values which do not change any more with increasing t.

3. Results and discussion

In Fig. 1, the scattered intensities from the microphase-separated melt of B100-3, B100-8, and B100-17 at approximately 65 °C are logarithmically plotted against s (closed circles). A couple of intensity maxima from the microdomain structure were observed, whose ratio exactly corresponds to $1 : \sqrt{3}$ for B100-3 and B100-8, which suggest the

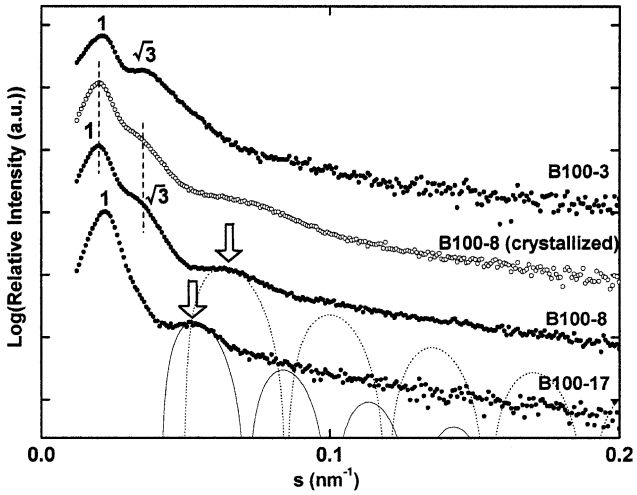

Fig. 1. Scattered intensity logarithmically plotted against s for the molten B100-3, B100-8, and B100-17 (closed circles) at approximately 65 °C and B100-8 crystallized at −45 °C (open circles). The dotted and solid curves are the best fit of Eq. (1) (only with respect to the peak position) for B100-8 and B100-17, respectively.

spherical microdomain structure considering the extremely small PCL fraction in the system. In addition, the scattered intensity curve has a broad scattering at an intermediate angle, which arises from the form factor of isolated PCL spheres in the system. The values of R_s and R_p can be independently evaluated by the methods described in Section 2. The scattering curves from isolated spheres reproduced by Eq. (1) are presented by dotted (for B100-8) and solid (for B100-17) curves in Fig. 1, where the arrow indicates the position used for fitting. The radii estimated by both methods are shown in Table 1, which agree satisfactorily with each other except for the case of B100-3, where the broad scattering is vague and the fitting procedure cannot be carried out. The agreement between R_s and R_p also suggests that the systems take spherical microdomain structures in the melt.

The SAXS curves for B100-8 in the melt (closed circles) and after crystallization at −45 °C (open circles) are similar in shape except that at intermediate angles; the angular positions of small-angle peaks for the crystallized B100-8 are identical with those for the molten B100-8 (indicated by vertical dotted lines), suggesting that the spherical microdomain structure is completely preserved after crystallization and therefore the PCL block crystallizes within the spherical microdomain. The change in SAXS curves at the intermediate angle will arise from the deformation of PCL spheres by crystallization, as pointed out by our group [7] and Loo et al. [2].

The crystallization of PCL blocks was confirmed by two methods: (1) observation of the exothermic peak by DSC when the sample is cooled from the microphase separated melt and (2) detection of characteristic reflections from PCL crystals. Fig. 2a shows the DSC curves when each sample is cooled from the melt at a rate of 5 °C/min. The curves for

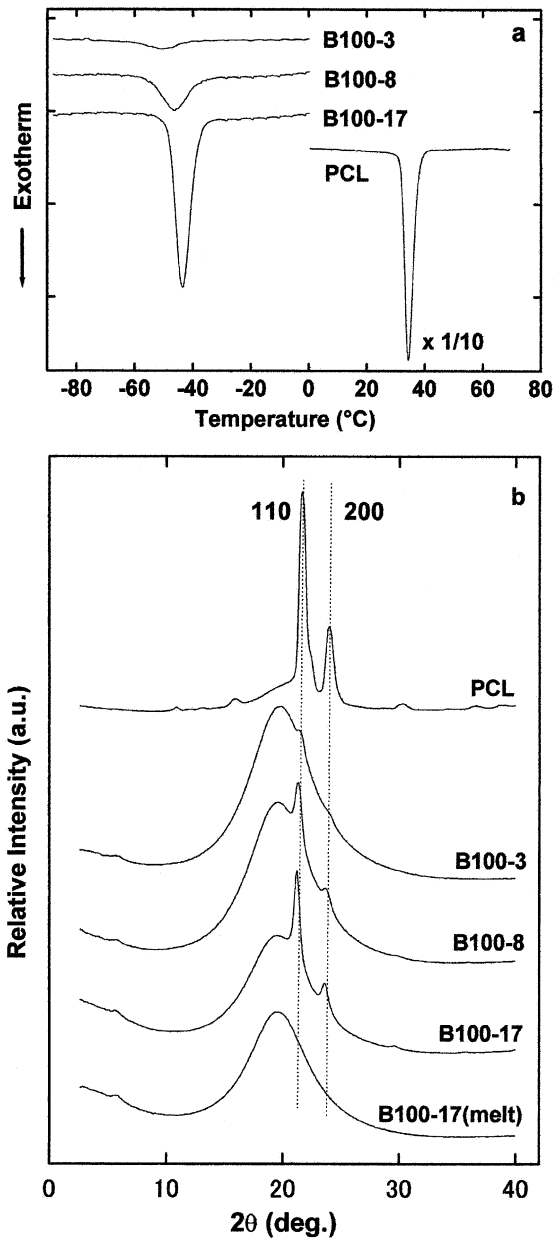

Fig. 2. (a) DSC exothermic curve when each sample is cooled at a rate of 5 °C/min. The DSC curve for PCL is reduced by a factor of 10 for clarity. (b) WAXD curve of each sample after crystallization. The bottom curve exhibits amorphous halo arising from the molten B100-7.

B100-3, B100-8, and B100-17 have an exothermic peak at −45 to −50 °C while that for PCL at 35 °C. The exothermic peak for PCL-*b*-PB indicates that PCL blocks certainly crystallize in the spherical microdomains. A large difference in the peak temperature between PCL and PCL-*b*-PB (80–85 °C) is already reported by Chen et al. [3] for the crystallization process starting from spherical or cylindrical microdomains formed in a poly(ethylene oxide)-*block*-polybutadiene copolymer. The large supercooling necessary for crystallization will be ascribed to the lack of nucleation opportunity, as discussed by Chen et al. [3,9]. Fig. 2b

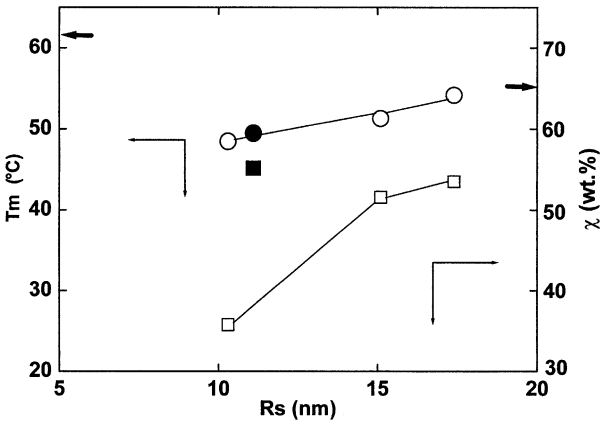

Fig. 3. T_m (open circle) and χ (open square) plotted against R_s for a series of PCL-*b*-PB with $M_n \approx 100{,}000$ crystallized at -45 °C. The closed symbols correspond to T_m and χ for B62-6 crystallized at -45 °C and the arrows represent those for PCL crystallized at 40 °C.

shows WAXD curves for the samples crystallized at 40 °C for PCL and -45 °C for PCL-*b*-PB. The bottom curve is from the molten B100-17 showing an amorphous halo without any reflection from PCL crystals. The WAXD curves for PCL-*b*-PB are the superposition of this amorphous halo mainly arising from amorphous PB blocks and the small crystallographic reflections from PCL crystals. These reflections can be successfully indexed as shown in Fig. 2b because the angular positions of reflections are exactly the same as those for PCL [10]. This indicates clearly that the PCL block crystallizes within spherical microdomains existing in the melt.

Fig. 3 shows the R_s dependence of T_m and χ for a series of PCL-*b*-PB with a same M_n (open symbols) and those for B62-6 (closed symbols) when they are crystallized at -45 °C. The arrows indicate T_m and χ for PCL crystallized at 40 °C. Though T_m and χ for PCL depend moderately on T_c, those for PCL-*b*-PB are hardly influenced by T_c ranging from -40 to -60 °C. This phenomenon is unique to the crystallization within microdomain structures. T_m decreases only slightly with decreasing R_s, suggesting that the lamella thickness within microdomains, which is fairly thinner than that of PCL, is almost constant irrespective of R_s. On the other hand, χ for PCL-*b*-PB is considerably lower than that of PCL (χ for B100-3 is, for example, about half of that for PCL) and decreases significantly with decreasing R_s. Intuitively, we can consider that χ for PCL is higher than that for PCL-*b*-PB because there is no specific restriction against the crystallization of PCL, while the curved interface of PCL spheres will extremely disturb the crystallization of PCL blocks. The volume fraction of curved interface regions that are not available for crystallization increases with decreasing R_s and eventually χ decreases steadily with decreasing R_s as shown in Fig. 3.

We find another fact by comparing the results of B62-6 with those of B100-3. Both have a similar R_s of PCL spheres (11.1 nm for B62-6 and 10.3 nm for B100-3), but χ for B62-6 is significantly higher than that for B100-3 though any significant difference in T_m cannot be found. This fact suggests that the crystallization in the spherical microdomain is not controlled only by the spherical size, but also by other factors such as the total molecular weight or the distance between neighboring spheres. This finding represents the complexity of crystallization of polymer chains confined within the nanospace. At present, we are studying the crystallization behavior of various PCL-*b*-PB to understand this complexity and the results will soon appear.

In summary, we studied the crystallization of PCL-*b*-PB which had spherical microdomain structures in the melt, and found that the PCL block certainly crystallized without destroying the existing microdomains. T_m decreased slightly but χ decreased significantly with decreasing R_s, which is intuitively understood by the difficulty of crystallization within the curved nanospace. However, we found that χ was significantly higher when the total molecular weight was reduced with R_s being constant. This fact suggests that the sphere size is not the unique factor to control crystallization. Other factors, combined with the sphere size, will cooperatively drive crystallization within the spherically confined nanospace.

Acknowledgements

This work was supported in part by Grants-in-Aid for Scientific Research on Basic Areas (C) (No. 12650879) and on Priority Areas (A), 'Dynamic Control of Strongly Correlated Soft Materials' (No. 413/13031035) from the Ministry of Education, Science, Sports, and Culture of Japan.

References

[1] Hamley IW. The physics of block copolymers. Oxford: Oxford University Press, 1998.
[2] Loo YL, Register RA, Ryan AJ. Phys Rev Lett 2000;84:4120.
[3] Chen HL, Hsiao SC, Lin TL, Yamauchi K, Hasegawa H, Hashimoto T. Macromolecules 2001;34:671.
[4] Nojima S, Kato K, Yamamoto S, Ashida T. Macromolecules 1992; 25:2237.
[5] Nojima S, Tanaka H, Rohadi A, Sasaki S. Polymer 1998;39:1727.
[6] Nojima S, Kikuchi N, Rohadi A, Tanimoto S, Sasaki S. Macromolecules 1999;32:3727.
[7] Nojima S, Hashizume K, Rohadi A, Sasaki S. Polymer 1997;38:2711.
[8] Crescenzi V, Manzini G, Calzolari G, Borri C. Eur Polym J 1970; 8:449.
[9] Chen HL, Wu JC, Lin TL, Lin JS. Macromolecules 2001;34:6936.
[10] Chatani Y, Okita Y, Tadokoro H, Yamashita Y. Polym J 1970;1:555.